

Invited

Intraband Relaxation Dynamics of Photo-Excited Carriers in GaAs and Related Compounds

C. L. Tang, F. W. Wise, and M. J. Rosker

Cornell University

Ithaca, NY 14853

Recent femtosecond optical studies of the intraband relaxation dynamics of photo-excited nonequilibrium carriers in GaAs, AlGaAs, and GaAs/AlGaAs multiple quantum well structures are reported. Improvements in time-resolution and sensitivity of our femtosecond measurement system have allowed for the first time extraction of the relaxation times corresponding to different scattering processes. Two or three distinct exponential decays are resolved for each material studied, with the fastest time constant measured to be approximately 40 femtoseconds.

With the current interest in ultra-high speed electronic and opto-electronic devices, it is important to understand the relaxation dynamics of non-equilibrium carriers in GaAs and related compounds. A variety of extremely fast and competing relaxation processes are involved. For electrons more than 0.3 eV above the band-edge in GaAs, for example, the relaxation time could be as fast as 30 femtoseconds. Until very recently, it had not been possible to measure such a short relaxation time directly. With the recent development of femtosecond lasers and related optic techniques, it is now possible to study such processes optically for the first time.

In what follows, we report our recent results on the relaxation dynamics of nonequilibrium carriers using the femtosecond transmission-correlation technique¹. In such experiments, the total power of two separate identical femtosecond laser pulses transmitted through a thin-layer of semiconductor is measured as a function of the delay between the two pulses. If the carriers generated by the two pulses see each other, there is a mutual saturation effect between the two pulses and, as a result, there will be an increase in the total transmitted power from that if the two pulses were far apart. As the delay between the two pulses increases beyond the carrier lifetime, the transmitted power levels off resulting in what is called transmission-correlation peak (TCP) near zero-delay.

The difference in the shape of the TCP and the autocorrelation trace of the incident pulses is a direct measure of the relaxation dynamics of the photo-excited carriers. The fastest process that we can now see with this method is about 25 fs, although the time-resolution in the case of slower processes is on the order of ± 4 fs. As an indication of the sensitivity of our system, our current signal-to-noise ratio is greater than 60 dB near the peak of the TCP. The degree of saturation at the peak is on the order of 1% of the total transmission through a typical sample of one attenuation length.

Fig. 1 shows the schematic of our experimental setup. The laser used was a modified colliding-pulse mode-locked dyelaser. This laser produces nearly transform-limited pulses as short as 40 fs with very clean profiles². Power spectrum of the pulses was peaked at about 630 nm with a pulse repetition range of 10^8 Hz.

Fig. 2 shows typical transmission-correlation traces obtained with four different types of samples: (1) a 300 nm thick layer of uncladded $\text{Al}_{0.32}\text{Ga}_{0.68}\text{As}$, (2) a layer of intrinsic GaAs 300 nm thick cladded by 150 nm layers of transparent (to 630 nm) $\text{Al}_{0.6}\text{Ga}_{0.4}\text{As}$, (3) a layer of GaAs of 1.3-micron thickness otherwise similar to the second sample, and (4) a MQW structure made of seven 145 Å thick GaAs layers alternating between 460 Å $\text{Al}_{0.6}\text{Ga}_{0.4}\text{As}$ barriers. All samples were grown using conven-

tional low-pressure MOCVD process, except for sample (3), which was grown using a standard LPE process. For all samples, the substrate was removed after growth in a 375-micron diameter circle via chemical etching. Unlike the other samples, sample (3) was optically thick (about 5 optical lengths), making interpretation of the result difficult. The wavelength of the fs laser pulses was always 630 nm.

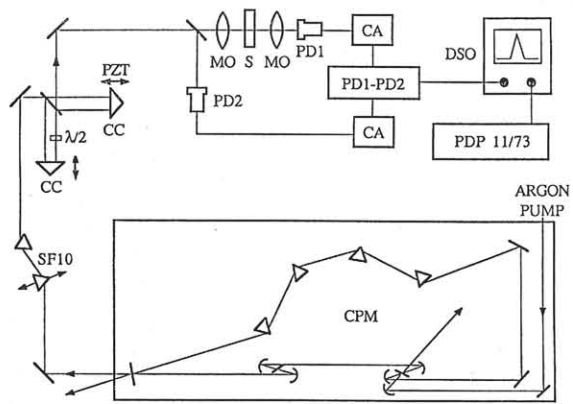


Fig. 1 - schematic of the experiment.
Key: CPM=Colliding-pulse mode-locked dye laser;
CC=corner -cube; $\lambda/2=\frac{1}{2}$ -wave plate; MO=micorscope
objective; S=sample; PD1,PD2=photociodes; PZT=
piezoelectric transducer; CA=current amplifier;
DSO=digital computer for signal averaging.

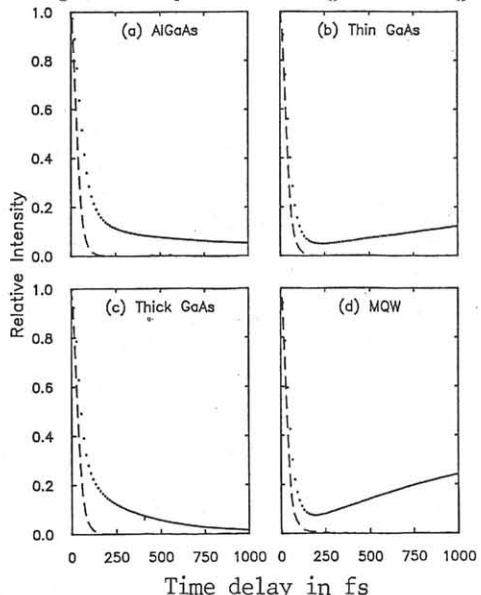


Fig.2 - Typical transmission-correlation
traces. See text for descriptions of samples.
The dashed lines are the pulse autocorrelation,
shown for reference.

For each case shown in Fig.2, the initial shape was found to be broader than the pulse auto-correlation trace (typically 40% greater in FWHM), indicating the presence of a fast (50 fs or less) decay mechanism. The TCP shapes in all cases also indicate additional slower processes. Exponential time constants were extracted from the data using a least-squares linear prediction (LP) algorithm³. In order to separate the response function from the effects of convolution with the source autocorrelation and the coherent artifact, all data for time delays less than 80fs (where the pulse autocorrelation falls to less than 5% of maximum) was excluded from LP fitting. Numerical simulation indicates that the largest error in estimated time constants introduced by non-response effects (convolution and coherent artifact) is less than 10%, although the possible error in amplitude estimates may be somewhat greater. The numerical fit unambiguously indicates the existence of two or three decay exponential components depending on the materials studied. The results are summarized in Table 1. In all the cases we studied, we did not see any obvious carrier density dependence. The range of density studied was from approximately 10^{18} to 10^{19} cm⁻³. The fact that no carrier-density dependence was seen could mean that either carrier-carrier scattering is insignificant or the carrier-density dependence of carrier-carrier scattering cancels that of the screening effect in the density range we studied.

Material	Polarization	Amplitude	Time Constant (fs)
Al _{0.32} Ga _{0.68} As		1.00	39.7 ± 1.8
		0.11	140 ± 20
		0.06	1650 ± 250
	⊥	1.00	45.6 ± 4.9
		0.16	145 ± 25
		0.08	1750 ± 200
GaAs (thin)		1.00	34.2 ± 1.2
		0.09	160 ± 30
		-0.11	1650 ± 50
	⊥	1.00	39.8 ± 2.1
		0.10	200 ± 45
		-0.14	1700 ± 300
GaAs (thick)		1.00	32.2 ± 1.5
		0.11	140 ± 20
		0.15	410 ± 20
MQW		1.00	45.0 ± 2.7
		-0.40	3000 ± 250

Table 1 - Amplitudes and time constants of exponential time constants deduced from the data shown in Fig. 2 through the linear prediction procedure³ for parallel and orthogonal polarizations of the incident pulses.

The interpretation of the physical origins of the observed exponential processes is still somewhat tentative. We believe that the observed time-dependence in the transmission characteristics reflects primarily the relaxation dynamics of the electrons photo-excited by the femtosecond pulses because of the large difference in the effective masses of the electrons and holes and the fact that the bandwidths of the excited carrier states are comparable to that of the photons. The measured value for the fast (approximately 40 fs) time constant is in reasonable agreement with the predicted¹ decay rate for deformation potential scattering of the electrons from the Γ -valley into the satellite valleys.

The intermediate decay component (approximately 150 fs) observed in the GaAs and AlGaAs samples is interpreted as due to polar-optical-phonon scattering within the Γ -valley. The measured value is again in reasonable agreement with theoretical estimates¹. The fact that we did not see this component in the MQW sample is interesting and possibly significant. Since in our experiment the excited electronic state is just above the bottom of one of the sub-bands of the quantized conduction band, the absence of an observable decay component due to polar optical phonon emission implies that the rate of decay between the sub-bands in quasi-two dimensional structures due to this mechanism is insignificant compared to that in the bulk GaAs. This may help to explain the previously unexplained effect^{4,5} that the cooling rate for hot carrier distributions in GaAs/AlGaAs quantum-well structures is significantly smaller than that in bulk GaAs for high carrier densities (10^{17} cm^{-3} or greater). This effect has never been satisfactorily explained, although a number of explanations have been suggested by various authors.

We have no explanation for the observed long decay component in AlGaAs. There are a number of possibilities, such as acoustic phonon scattering or alloy scattering¹. The long rising components (picosecond or longer) observed in the thin GaAs and MQW samples have been observed before⁶ and was explained as due to saturation of the split-off transition in GaAs which is not present in AlGaAs for 2 eV photons.

In conclusion, we have measured the decay of photoexcited populations in GaAs, $\text{Al}_{0.32}\text{Ga}_{0.68}\text{As}$, and GaAs/AlGaAs multiple quantum wells. We have found the initial exponential decay for each of these materials to be dominated by an approximately 40 fs component. We have also resolved either one or two other characteristic time constants for each of these materials between a hundred femtoseconds to a few picoseconds.

This work was supported by the National Science Foundation and JSEP. The manuscript was completed while one of the authors (CLT) was a Visiting Researcher at the NTT Basic Research Laboratory, Musashino-Shi, Japan. He would like to thank his colleagues in this laboratory for their hospitality.

REFERENCES

1. A. J. Taylor, D. J. Erskine, and C. L. Tang, JOSA B, Vol. 2, 663(1986).
2. J. A. Valdmanis, R. L. Fork, and J. P. Gordon, Opt. Lett., Vol. 10, 131(1985).
3. H. Barkhuijsen, R. De Beer, W. M. M. J. Bovee, and D. Van Ormondt, J. Mag. Res., Vol. 61, 465 (1983).
4. Z. Y. Xu and C. L. Tang, App. Phys. Lett. Vol. 44, 692(1984).
5. J. F. Ryan, R. A. Taylor, A. J. Turberfield, A. Maciel, J. M. Worlock, A. C. Gossard, and W. Wigman, Phys. Rev. Lett. Vol. 53, 1841(1984).
6. A. J. Taylor, D. J. Erskine, and C. L. Tang, App. Phys. Lett., Vol. 45, 1209(1984).

